NANO LETTERS

Letter

Nanoscale Patterns of Oligonucleotides Formed by Electrohydrodynamic Jet Printing with Applications in Biosensing and Nanomaterials Assembly

Jang-Ung Park, Jung Heon Lee, Ungyu Paik, Yi Lu, and John A. Rogers

Nano Lett., **2008**, 8 (12), 4210-4216 • Publication Date (Web): 29 October 2008

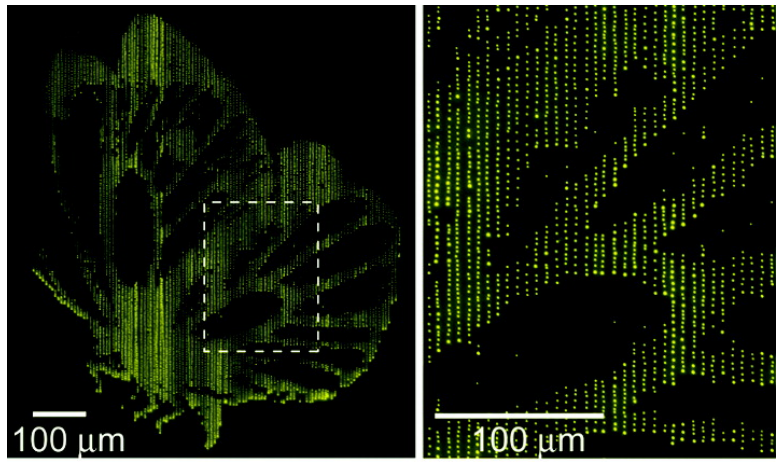

More About This Article

Additional resources and features associated with this article are available within the HTML version:

- Supporting Information
- Access to high resolution figures
- Links to articles and content related to this article
- Copyright permission to reproduce figures and/or text from this article

View the Full Text HTML

Nano Letters is published by the American Chemical Society. 1155 Sixteenth Street N.W., Washington, DC 20036

NANO LETTERS

2008
Vol. 8, No. 12
4210-4216

Nanoscale Patterns of Oligonucleotides Formed by Electrohydrodynamic Jet Printing with Applications in Biosensing and Nanomaterials Assembly

Jang-Ung Park,[†,‡] Jung Heon Lee,[†,‡] Ungyu Paik,[⊥] Yi Lu,[*,‡,§,||] and John A. Rogers[*,‡,§]

Department of Materials Science and Engineering, Beckman Institute for Advanced Science and Technology, Frederick Seitz Materials Research Laboratory, Department of Chemistry, Department of Biochemistry, and Center for Biophysics and Computational Biology, University of Illinois at Urbana−Champaign, Urbana, Illinois 61801, and Division of Advanced Materials Science Engineering, Hanyang University, Seoul, Korea

Received June 25, 2008; Revised Manuscript Received September 19, 2008

ABSTRACT

The widespread use of DNA in microarrays for applications in biotechnology, combined with its promise in programmed nanomaterials assembly, unusual electronic devices, and other areas has created interest in methods for patterning DNA with high spatial resolution. Techniques based on thermal or piezoelectric inkjet printing are attractive due to their noncontacting nature and their compatibility with diverse materials and substrate types; their modest resolution (i.e., 10−20 μm) represents a major limitation for certain systems. Here we demonstrate the use of an operationally similar printing approach that exploits electrohydrodynamic forces, rather than thermal or acoustic energy, to eject DNA inks through fine nozzles, in a controlled fashion. This DNA printer is capable of resolution approaching 100 nm. A range of experiments on patterns of DNA formed with this printer demonstrates its key features. Example applications in DNA-directed nanoparticle assembly and DNA aptamer-based biosensing illustrate two representative uses of the patterns that can be formed.

Deoxyribonucleic acid (DNA) microarrays are of great interest for genomics and medical diagnostics, due to their utility for rapid identification of gene expressions and disease states. Such microarrays consist of arrangements of multiple DNA probe sites on a surface.[1] Each site bears a reagent whose molecular recognition of an analyte (cDNA strand, inorganic ion, organic small molecule, virus, cancer cell, etc.) can produce a signal suitable for detection by an imaging technology, most often fluorescence. The total number of probe sites (dots) determines the number of recognition possibilities that can be evaluated; the size of these dots determines the volume of the analyte required. As a result, a key metric for such microarrays is the number of dots per unit area. An important goal, then, is to pattern, at high speed, dots of DNA with sizes and spacings comparable to the detection limits of conventional fluorescence imaging techniques (dimensions ∼ (emission wavelength)/2). These microarrays, together with emerging uses of DNA in biosensing,[2−5] nanomaterials assembly,[6−12] nanoelectronics,[13] and other fields, motivate the development of techniques for high-resolution patterning of DNA and related classes of biomaterials.

One of the first demonstrations of DNA printing used arrays of pins, as a kind of stamp, to form microarrays. Although this initial work[14] involved relatively large dot sizes and spacings (∼270 and 500 μm, respectively), replacing the pins with true, high-resolution stamps[15−20] enables features with sizes of ∼40 nm.[15,16] A drawback is that specific interactions for (i) adsorption of DNA on the stamp and (ii) transfer from the stamp to the substrate are typically necessary. Examples include hydrogen bonding[15−17] and hydrophobic[18] or electrostatic interactions.[19,20] Also, the materials utilization is poor because although the entire area of the stamp is inked with DNA, only a fraction of this ink, corresponding to that on the raised regions, is printed. Writing with continuous scanning tips provides a different,

* To whom correspondence should be addressed. E-mail: yi-lu@illinois.edu (Y.L.); jrogers@illinois.edu (J.A.R.).
† J.-U. Park and J. H. Lee contributed equally to this work.
‡ Department of Materials Science and Engineering, Beckman Institute for Advanced Science and Technology, and Frederick Seitz Materials Research Laboratory, University of Illinois at Urbana−Champaign.
§ Department of Chemistry, University of Illinois at Urbana−Champaign.
|| Department of Biochemistry and Center for Biophysics and Computational Biology, University of Illinois at Urbana−Champaign.
⊥ Division of Advanced Materials Science Engineering, Hanyang University.

10.1021/nl801832v CCC: $40.75
Published on Web 10/29/2008

but related, type of contact-based patterning modality. One of the most prominent such techniques is dip-pen nanolithography (DPN), in which atomic force microscopy (AFM) tips directly write patterns of DNA with sizes down to sub-50 nm (spacings ~1 μm).[21,22] Current DPN research focuses on the development of integrated microfluidic systems to eliminate the need for multiple inking steps and of massively parallel arrays of tips and motion control systems to increase patterning speeds and areas.[23] A technique conceptually related to the microfluidic embodiment of DPN uses pipets[24,25] with ~100−200 nm inner diameter (i.d.) and ~100 nm standoff-height to form dots of DNA with ~400 nm diameters and ~1 μm spacings. This process, as with DPN, works best with DNA that is functionalized to bind to the substrate (e.g., thiolated DNA on gold substrates) or that incorporates other specific DNA−substrate interactions to facilitate transfer.

Approaches that remove the requirements for intimate/proximal contact and for DNA/substrate bonding are of interest. The most well developed examples involve adaptations of inkjet printing techniques[26−29] and electrohydrodynamic jet/spray methods.[30,31] These noncontact strategies print DNA onto the substrate, from distances of 100 μm or more, in the form of liquid jets or sprays of droplets. This patterning geometry achieves low levels of contamination, high throughput, compatibility with large area substrates, with nearly any combination of biomaterial ink and substrate. In fact, DNA microarrays formed by piezoelectric inkjet printing are now commercially available.[27] A primary disadvantage of these methods is that their resolution is modest; DNA dots with controlled sizes and spacings less than ~10 μm have not been reported. Although electrospray[30,32] can generate comparatively smaller droplets, it produces patterns with broad and nonuniform size distributions. Here, we introduce the use of a high-resolution electrohydrodynamic jet (e-jet) printing technique to form dots of diverse types of single- and double-stranded DNA with diameters less than 100 nm, in arrays and other various complex patterns. Immobilization and hybridization of e-jet printed DNA using standard fluorescence tagging techniques demonstrate their suitability for use in microarrays. The implementation of high-resolution printed patterns of DNA for adenosine biosensors and templated nanomaterial assembly illustrate other potentially important classes of application.

E-jet printing uses electric fields to form micrometer and submicrometer sized droplets with micro/nanocapillary nozzles. Figure 1 schematically illustrates a printing system based on this approach,[33,34] configured to print suspensions of DNA in aqueous buffer solutions (typically 50 mM NaCl/25 mM potassium phosphate, pH 6.9). The addition of a small amount of glycerin (10 vol %) to these DNA inks prevented drying-induced clogging of the nozzles and enhanced the stability against electrical discharge (dielectric strength of glycerin is much larger than that of water). Supplementary Table 1 provides the sequences of DNA used in this paper (see Supporting Information). Glass capillaries with 2 μm i.d. or 500 nm i.d. served as the nozzles. A thin coating of gold (~50 nm thickness) with an Au/Pd adhesive layer (~30

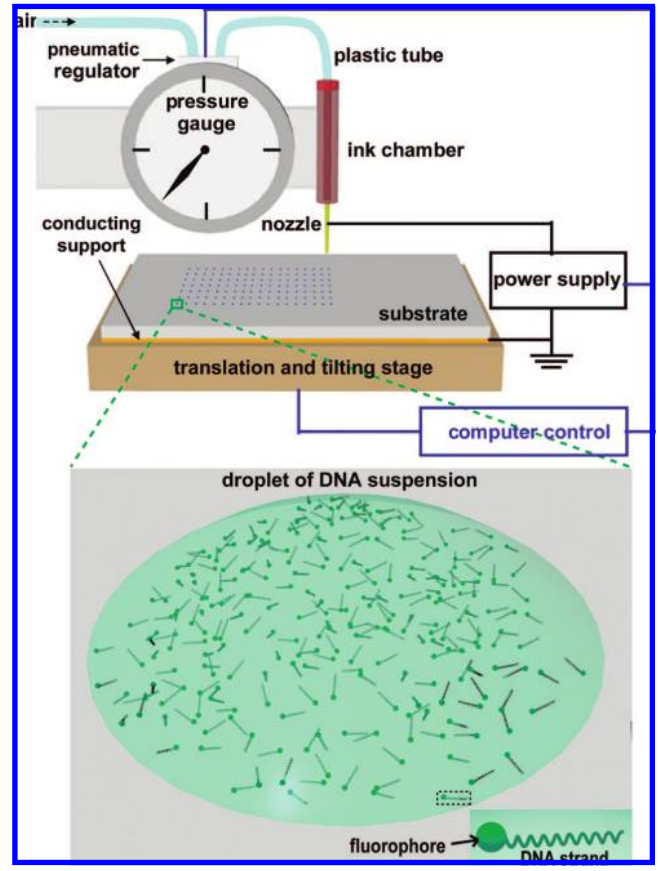

Figure 1. Schematic diagram of a high-resolution, electrohydrodynamic jet (e-jet) printing system. Aqueous suspensions of single-stranded (ss) or double-stranded (ds) oligonucleotides can be printed on a substrate using such an e-jet printer.

nm thickness) on the entire outer surface and the inner surface near the tip provided electrical contact to the ink. A hydrophobic self-assembled monolayer (1*H*,1*H*,2*H*,2*H*-perfluorodecane-1-thiol) on the gold prevented unwanted wetting of the inks with the outer part of the tip. The ink flowed to the nozzle tip through the application of constant pressure to a connected reservoir by use of a regulated supply of compressed air. For the setups used here, a pendent meniscus formed at the nozzle tip upon application of a pressure of ~2 psi, for nozzles with 2 μm or 500 nm i.d. The substrate for printing was mounted on a computer-controlled air-bearing translation stage below the nozzle tip with a standoff height of ~30 μm. A cooled CCD camera (Infinity 3, Lumenera Corp.) and long working distance optics provided an ability to view the printing process at high magnification. Applying an electric field between the nozzle tip and wafer created electrostatic stresses associated with Coulombic repulsion between mobile charges in the ink, mostly ions in the buffer solution. These stresses deformed the meniscus into a conical shape, known as a Taylor cone.[35] With further increases in voltage, the sum of the forces associated with the applied pressure and electrostatics exceeded those associated with the capillary pressure, thereby forming a liquid jet that ejected from the apex of the cone toward the substrate.[36] After an ejection, the jet recoiled back to the nozzle tip, leaving a droplet on the substrate. With a constant, time-invariant voltage in this range, the jet was observed to

pulsate in a manner that produced printed dots with spatial layouts defined by computer control of the voltage and the substrate stage. This printing process used jet pulsation frequencies of a few hertz to allow easy observation with the CCD camera (15 frames per second). Pulsation rates as high as a few kilohertz were possible with increased applied voltage.[36] Two printing modes are possible. In the first, the system prints at a characteristic frequency as the nozzle scans over the substrate. In this case, the positions of individual droplets are not well controlled. In the second, the driving voltage is turned on and off such that ejection of each individual droplet is under direct computer control. This "drop-on-demand" mode provides excellent control over the placement of individual droplets, although in its current implementation it offers lower printing speeds than the first mode.

As an example of capabilities in e-jet printing of DNA, Figure 2a presents an optical micrograph of a dot matrix butterfly pattern formed using the first printing mode with an ink of a single-stranded DNA (ssDNA, 5 μM), fluorescently labeled with Alexa546 (emission wavelength 573 nm) [ss-butterfly]. Alexa546 was chosen for its high quantum yield and photostability.[37] This pattern used a nozzle with 2 μm i.d. to achieve dot sizes of $\sim$2 μm spaced by distances of $\sim$6 μm in horizontal rows and $\sim$4 μm in vertical rows. The spacings of the horizontal rows were selected by the user upon conversion of an original image file (in JPG format) to the g-code that controls the printer machine. The intrinsic pulsation frequency ($\sim$5 Hz) and the translation speed of the stage (20 μm/s) defined the spacings in the vertical rows. (Similar dot sizes and spacings can be printed at increased pulsation frequencies and translation speeds. The alphabetic letters "UIUC" in Supplementary Figure 1 were printed with similar dot sizes and spacings ($\sim$3 μm in diameter and $\sim$6 μm in spacing) at 10 times increased pulsation frequency and translation speed ($\sim$50 Hz and 200 μm/s).) Supplementary Movies 1 and 2 show the printing processes with the speeds of 20 and 200 μm/s, respectively. As an example of the drop-on-demand e-jet printing, 14 $\times$ 14 arrays of the DNA dots were printed using the pulse bias (1.2 s width, 1.7 s period), as shown in Figure 2c. Here, the positions of individual droplets are controlled to a precision of $\pm$0.3 μm. The spacing, and more generally the positioning of each dot, can be selected by user. As an example, a square array of dots with 10 μm spacing and the same dot sizes appear in Supplementary Figure 2. This DNA dot size is roughly 10 times smaller than that achieved with conventional inkjet systems.[26−29] Even at these small dimensions, the intensity of the fluorescence is readily detectable with standard fluorescence imaging microscopes (see Supporting Information). Figure 2b shows a fluorescence micrograph of the same pattern in Figure 2a. The sizes of the dots can be substantially reduced by decreasing the inside diameters of the nozzles. For example, Figure 2d presents AFM images of dots with $\sim$100 nm diameters, e-jet printed using a nozzle with a 500 nm i.d. This feature size approaches that achieved with DPN. Although it has limited utility for DNA microarrays because the associated fluorescence from a single dot is too small to be detected effectively using conventional systems, such resolution can be important for fundamental study of molecular interactions at nanometer scales or for applications such as nanomaterials assembly, as described subsequently, and unusual electronic devices.

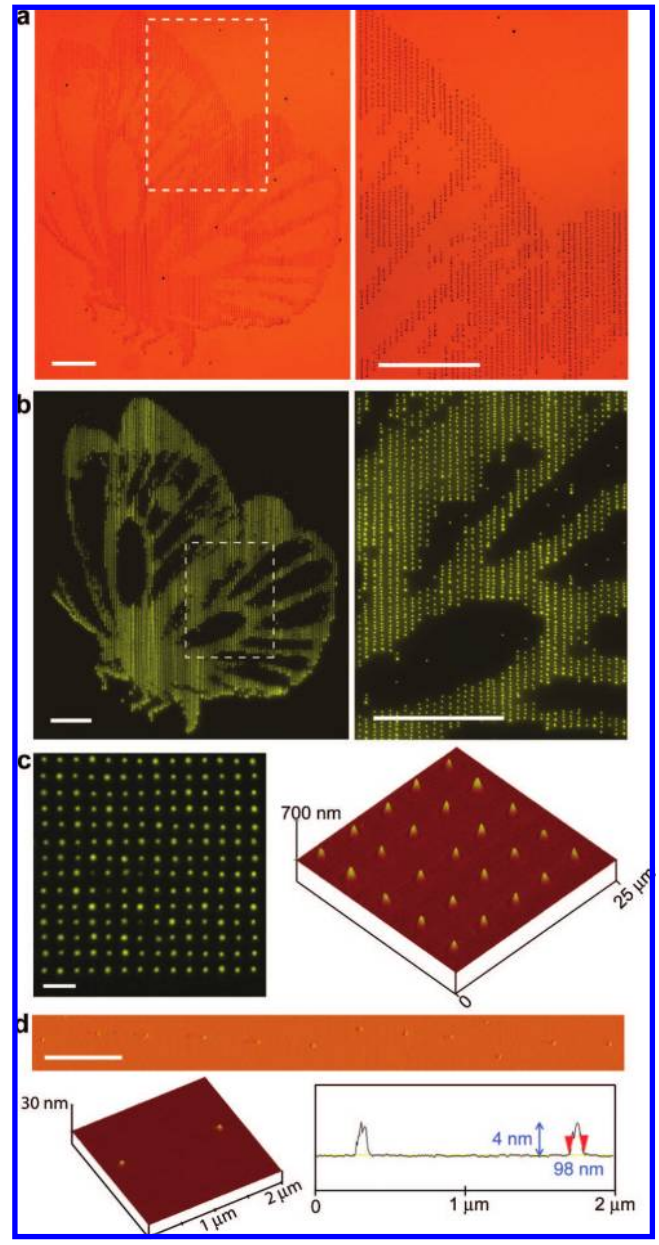

Figure 2. Images of patterns of DNA formed by e-jet printing. (a) Optical and (b) fluorescence micrographs of a butterfly pattern, e-jet printed onto a Si wafer using an oligonucleotide suspension (37-mer ssDNA labeled with Alexa546) and a nozzle with a 2 μm i.d. As shown in the magnified images (right), this pattern is composed of arrays of dots $\sim$2 μm in diameter. Scale bars are 100 μm. (c) fluorescence micrograph (left) and AFM image (right) of DNA microarrays (37-mer ssDNA labeled with Alexa546), printed in the drop-on-demand mode using a 2 μm nozzle. Dot diameters and spacings are $\sim$2 and 5 μm, respectively. The scale bar is 10 μm. (d) AFM image of dots printed using an oligonucleotide suspension (37-mer ssDNA, 1 μM in 100 μM K-phosphate buffer) and a nozzle with a 500 nm i.d. The average dot diameter is $\sim$100 nm. Scale bar indicates 2 μm. Three dimensional rendering of an AFM image (bottom left) and a height profile (bottom right).

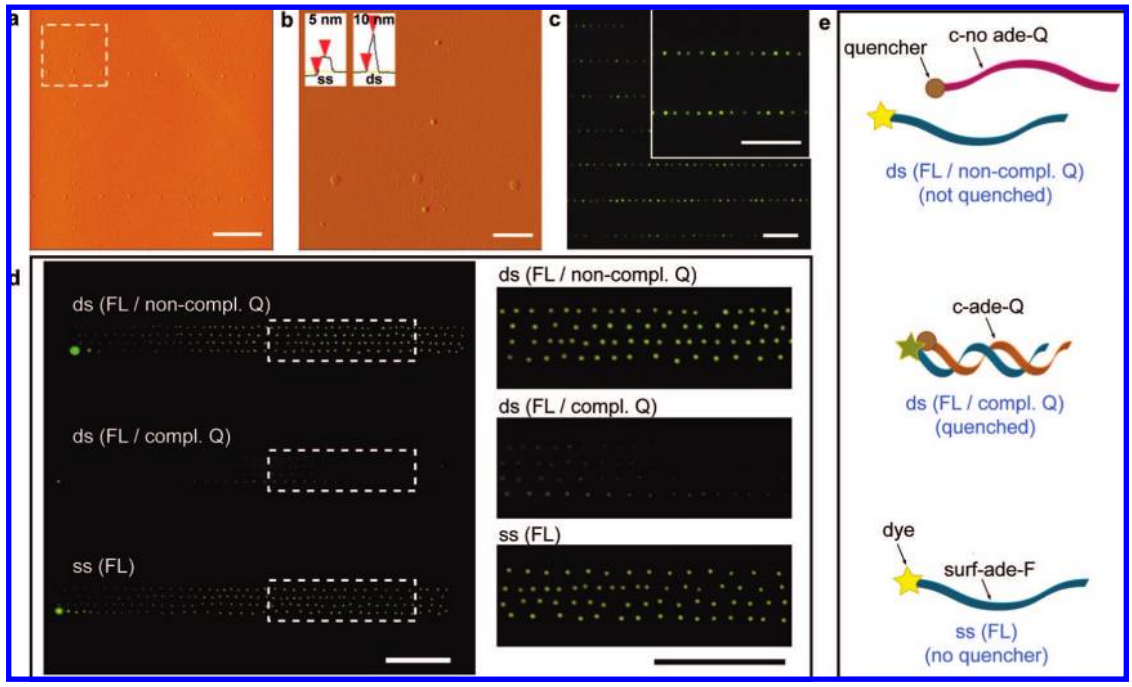

Figure 3. Studies suggesting that e-jet printing of dsDNA does not cause denaturation. (a) AFM image of dots printed using suspensions of ssDNA (dots in horizontal rows) and dsDNA (dots in vertical lines). The ssDNA (42-mer, 2 μM) is labeled with a fluorophore [ss (FL)]. The dsDNA consists of the same ssDNA hybridized to a complementary strand that contains a quencher [ds (FL/compl. Q)]. Scale bar is 20 μm. (b) Magnified view of white-dashed square area in (a). Dots of the ssDNA and dsDNA are ~1.2 μm in diameter (~5 nm in height) and ~800 nm in diameter (~10 nm in height), respectively. Scale bar indicates 5 μm and the insets show height profiles. (c) Fluorescence micrograph of the pattern of (a). The intensity observed from the ssDNA dots is significantly higher than that from the dsDNA dots, indicating that the quencher remains in close proximity to the fluorophore in this case, consistent with maintained hybridization. Scale bars are 50 μm. (d) Fluorescence micrographs of arrays of dots of ss (FL), ds (FL/compl. Q), and ds (FL/ noncompl. Q). Dot sizes are ~2 μm in diameter for the three cases. Since the noncomplementary strand is not hybridized, the fluorescence intensity of the ds (FL/noncompl. Q) dots is comparable to that of ss (FL). Scale bars present 50 μm. (e) Schematic illustrations for ss (FL), ds (FL/compl. Q), and ds (FL/noncompl. Q).

Compared to ssDNA, double-stranded DNA (dsDNA), particularly at short lengths, can potentially be denatured by the temperatures, pH levels, and shear rates[38] that can occur in certain printing processes, particularly with thermal inkjet[38,39] and electrospray.[32,38] Systematic experiments reported here indicate an ability to pattern dsDNA by e-jet, without significant denaturing. In one case, e-jet printing of 2 μM dsDNA (37 base pairs) that incorporated one strand labeled with a fluorophore and its complementary strand labeled with a quencher [ds (FL/compl. Q)], using a nozzle with 2 μm i.d. at a pressure of ~1.5 psi yielded a pattern of dots in a vertical array (Figure 3, panels a and b). A similar, but horizontally oriented, pattern of dots of 2 μM ssDNA (42-mer) labeled with a fluorophore [ss (FL)], was then printed on the same substrate with the same setups and conditions. (The dot sizes are ~1 μm in diameter and ~5−10 nm in height. The slight variation of the dot sizes for the two cases is related to finite tolerances in the applied pressure (±0.2 psi), nozzle size (±0.4 μm), and standoff height (±2 μm).) Figure 3c presents a fluorescence micrograph of this sample. In hybridized [ds (FL/compl. Q)], the fluorophore and quencher are sufficiently close in distance that efficient energy transfer occurs between them, thereby significantly reducing the fluorescence compared to that of the fluorophore without the quencher. As shown in Figure 3c, the fluorescence of the dsDNA dots (in vertical rows) is much weaker than that of the ssDNA dots (in horizontal rows). This result suggests that dsDNA can be e-jet printed without significant denaturing. We speculate that the screening provided by the positively charged ions in the buffer prevents denaturing that otherwise might be expected to occur due to Coulombic repulsive forces between negatively charged DNA backbones. For further comparison, 5 μM nonhybridized dsDNA that incorporated one strand with the fluorophore and a noncomplementary strand with the quencher [ds (FL/noncompl. Q)] was printed together with 5 μM [ss (FL)] and 5 μM [ds (FL/compl. Q)], as shown in Figure 3d. Dots of [ds (FL/noncompl. Q)] had similar fluorescence intensity to those of [ss (FL)]; both were brighter than [ds (FL/compl. Q)]. These results provide additional evidence that the observed quenching arises from hybridization that is not disrupted by printing.

E-jet printing can be performed using either positive or negative polarity of the electric field. This parameter did not affect the dot size or hybridization of [ds (FL/compl. Q)], as shown in Supplementary Figure 3. Tests that involved printing of the buffer solution onto pH test paper (Micro Essential Laboratory, pH indication range 1−11) showed negligible changes in pH in the range of 5−7 with polarity.

Many of the capabilities of e-jet printing of DNA well match the requirements for microarrays. Although microarrays are typically used to recognize the sequences of

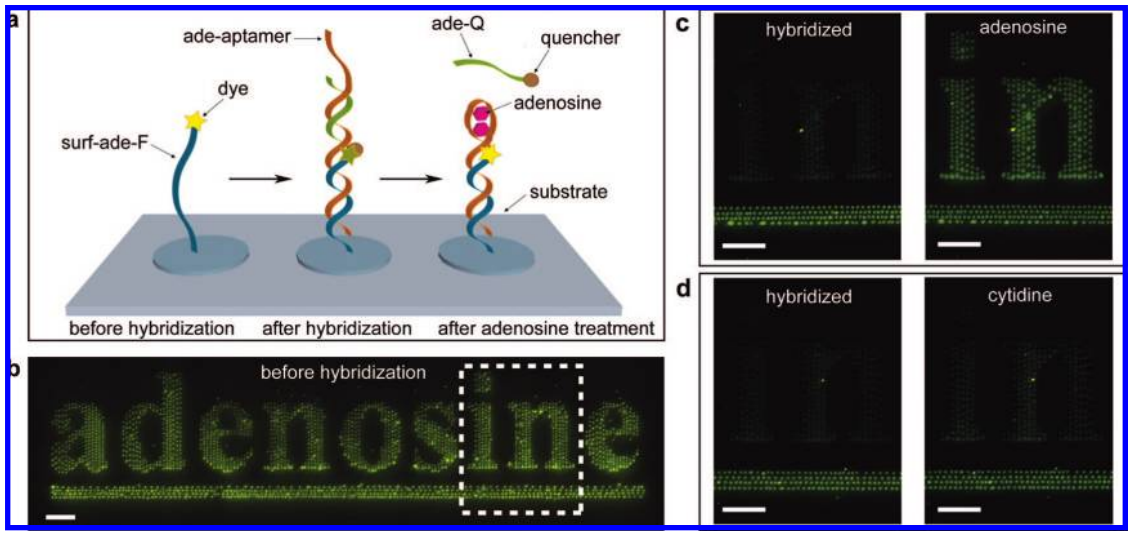

Figure 4. Aptamer-based biosensor for adenosine, patterned by e-jet printing. (a) Schematic representation of the detection of adenosine using e-jet printed aptamer patterns. (b) Fluorescence micrograph of the letters printed with [surf-ade-F] and underline with [surf-no ade-F] as an internal control. (c) Fluorescence micrographs of the pattern after (i) hybridization with two complementary strands (ade-aptamer and ade-Q), and (ii) reaction with adenosine molecules. (d) Fluorescence micrographs of the pattern after (i) hybridization with the same two complementary strands and (ii) reaction with cytidine, for comparison with the adenosine case. Scale bars in (a−d) are 50 μm.

unknown strands for genomics,[1] recent advances in selection of functional DNA (including DNAzymes, aptamers, and aptazymes) extend the possibilities to the detection of broad ranges of analytes, such as inorganic ions, small organic molecules, cancer cells, or viruses, all with high selectivities.[40−44] In particular, DNA aptamers selected by in vitro selection methods (SELEX) represent an interesting class of functional DNAs that binds only to specific molecules.[40,41] A growing number of reports describe the selection of new aptamers and their use in biosensors to detect, as examples, adenosine, cocaine, or thrombin.[45,46] Immobilized aptamer microarrays represent an advanced implementation, suitable for sensing multiple analytes simultaneously.[47] Such systems, like conventional microarrays, benefit from small dots and large numbers of dots per unit area. As a demonstration, we used e-jet printing to form a simple type of adenosine−aptamer microarray, patterned into a complex geometry, as a fluorescence biosensor for adenosine. We used biotinylated strands with streptavidin-coated substrates to immobilize the e-jet printed DNA. (More detail information on this immobilization process is described in our Supporting Information.) First, 5 μM ssDNA with biotin modification on the 3′ end and alexa546 modification on the 5′ end [surf-ade-F] was printed onto a streptavidin-coated Si substrate (SiO_2 thickness 20 nm), as illustrated in Figure 4a, in alphabetic patterns composed of dots with ∼3 μm diameters. These letters as well as an internal control, the line printed underneath the letters with [surf-no ade-F] strand at the same condition, are all brightly visible in the fluorescence micrograph of Figure 4b. After unreacted streptavidin was inactivated on the unprinted regions with a blocking buffer, two strands of DNA consisting of (i) one complementary to [surf-ade-F] but with an adenosine specific aptamer part on the elongated 3′ end [ade-aptamer] and (ii) its 12-mer partial complement, with a quencher label on its 3′ end [ade-Q] were hybridized with the originally printed strand [surf-ade-F]. This hybridization quenched the fluorescence of the letters, thereby darkening the image pattern in comparison to the internal control (left insets in Figure 4, panels c and d). Exposure to an aqueous solution of adenosine (2 mM) for only 30 s causes structure switching of the aptamer strand and release of the strand [ade-Q],[50] resulting in increased fluorescence signal again (right image in Figure 4c; for detailed illustration of adenosine-induced structure switching of the aptamer strand, see Supplementary Figure 5). To demonstrate the selectivity of this printed biosensor, the same experiments were carried out with cytidine, instead of adenosine. As shown in Figure 4d (right inset), the fluorescence intensity did not change significantly with this exposure, consistent with a negligible interaction between the aptamer and cytidine. This device therefore works as a turn-on sensor for adenosine. We expect, in fact, that the e-jet printing technique can be applied for sensing a number of other analytes using different aptamers, for example which specifically interact with other small molecules, proteins, or cells.

In addition to microarrays and sensors, e-jet printed DNA can act as templates for selective assembly of different nanoparticles (NPs) by exploiting the hybridization interactions between DNA strands.[49,50] For this demonstration, first, 5 μM of two noncomplementary DNA strands [surf-ade-F] and [surf-no ade-F], both with alexa546 modification on 5′ end and biotin modification on 3′ end, were printed on a Si wafer (with streptavidin top surface) using 2 μm i.d. nozzles to write the letters "A" and "B", respectively. Similar to an aptamer-based sensing system, we used biotinylated strands with streptavidin-coated substrates to immobilize the e-jet printed DNA. A fluorescence micrograph of a printed sample is shown in Figure 5a. Next, the unreacted streptavidin groups on the unprinted areas were inactivated using a blocking buffer. To allow the assembly of AuNPs on the letter "A" only, this sample was incubated in a solution of AuNPs (13 nm in diameter) functionalized with DNA [c-ade-Au]

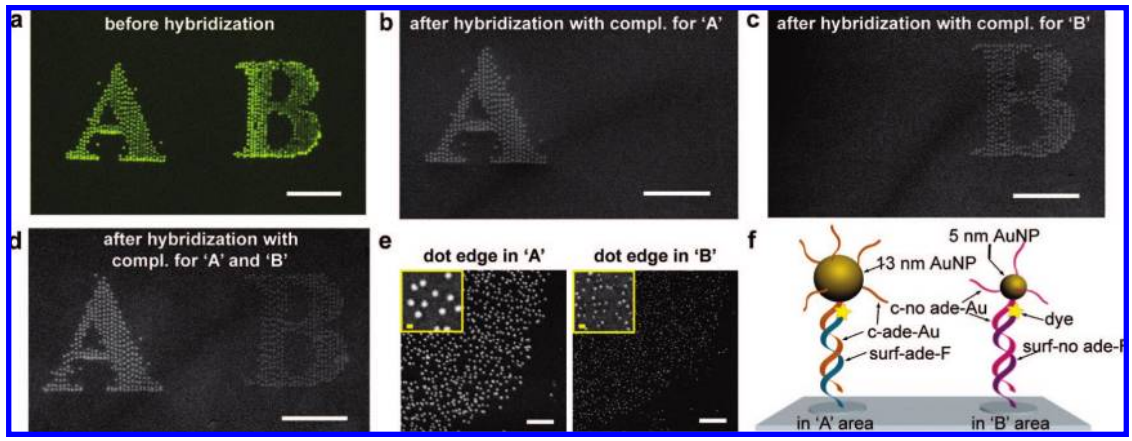

Figure 5. Selective AuNP assembly using DNA hybridization and e-jet printing. (a) Fluorescence micrograph of the e-jet printed letters "A" and "B" using two ss (FL) strands with different sequences. (b) SEM image of 13 nm-AuNPs selectively assembled on "A". AuNPs are conjugated to DNA complementary to the strand used to print "A". (c) SEM image of 13 nm AuNPs selectively assembled on "B". AuNPs are conjugated to DNA complementary to the strand used to print "B". (d) SEM image of 13 and 5 nm AuNPs selectively assembled on "A" and "B", respectively. AuNPs of 13 nm and 5 nm are conjugated to DNA complementary to the strand used to print "A" and "B", respectively. Scale bars in (a−d) are 100 μm. (e) SEM images of the magnified areas at the dot edges of "A" and "B" with scale bars of 200 nm. Yellow scale bars in the left-top insets indicate 15 nm. (f) Schematic illustration for the AuNP−DNA assembly formations on the "A" and "B" sites.

complementary to the strand [surf-ade-F] used to print the letter "A". The AuNPs selectively assembled on the letter "A", and not on "B"; only the letter "A" is visible in the SEM image (Figure 5b). To demonstrate that the assembly is sequence specific, the same experiment was carried out in a solution of AuNPs (with the same diameter) functionalized with DNA [c-no ade-Au] complementary to [surf-no ade-F] used to print the letter "B". In this case, only the letter "B" appears in the SEM image (Figure 5c), consistent with selective binding at the expected locations.

To demonstrate the assembly of two different nanoparticles in a one-pot process, a mixture of (i) 13 nm AuNPs functionalized with the strand [c-ade-Au] (complementary to the DNA printed for letter "A") and (ii) the 5 nm AuNPs functionalized with [c-no ade-Au] (complementary to the strand printed for letter "B") were used for the incubation, and the same experiment was carried out again. As shown in the SEM image (Figure 5d), both letters "A" and "B" are visible with difference in brightness due to the size difference of assembled NPs. The magnified images of the dot areas in patterns "A" and "B" are presented in Figure 5e. Thirteen nm AuNPs are mostly placed on the letter "A" while 5 nm AuNPs are on the "B", which proves nanomaterials can selectively bind on preassigned locations (e-jet printed areas) by their specific sequences. In the SEM image, the densities of NPs (the number of NPs per area) are ~550 and ~ 1000 NPs/μm^2 for the "A" and "B", respectively. Since each NP is functionalized with multiple strands, Coulombic repulsive forces between negatively charged individual NPs may limit the density.

In summary, the results presented here demonstrate the ability to print, in a controlled fashion, submicrometer sized droplets of various forms of DNA, by use of electrohydrodynamic effects at the electrically biased tips of fine nozzles. The experimental data, such as fluorescence based binding assays, indicate that the properties of DNA are not adversely affected by this printing process. Large scale patterns of DNA with complex geometries and feature sizes in the submicrometer range can be formed readily, suitable for use in not only the NP assembly templates and biosensors described here but also in other application areas. Exploring these possibilities and further developing the printing techniques by, as examples, implementing large scale arrays of nozzles for high-speed patterning and refining biasing conditions for drop-on-demand operation, all appear to be promising directions for future work.

Acknowledgment. This work was supported by the Center for Nanoscale Chemical Electrical Mechanical Manufacturing Systems at the University of Illinois (funded by the National Science Foundation under Grant DMI-0328162) and by the Korean Foundation for International Cooperation of Science and Technology (KICOS) through a grant [K2070400000307A-050000310, Global Research Laboratory (GRL) Program] provided by the Korean ministry of Science and Technology (MOST) in 2007. The general characterization facilities were provided through the ITG group and the Materials Research Laboratory with support from the University of Illinois and from Department of Energy Grants DE-FG02-07ER46453 and DE-FG02-07ER46471. We thank Jon Ekman for his assistance with fluorescence imaging.

Supporting Information Available: Supplementary figures showing printing results, experimental details, and movies of the printing processes. These materials are available free of charge via the Internet at http://pubs.acs.org.

References

(1) Pirrung, M. C. *Angew. Chem., Int. Ed.* **2002**, *41*, 1276–1289.
(2) Li, J.; Lu, Y. *J. Am. Chem. Soc.* **2000**, *122*, 10466–10467.
(3) Patolsky, F.; Lichtenstein, A.; Willner, I. *Nat. Biotechnol.* **2001**, *19*, 253–257.
(4) Ke, Y.; Lindsay, S.; Chang, Y.; Liu, Y.; Yan, H. *Science* **2008**, *319*, 180–183.

(5) Navani, N. K.; Li, Y. *Curr. Opin. Chem. Biol.* **2006**, *10*, 272–281.
(6) Mirkin, C. A.; Letsinger, R. L.; Mucic, R. C.; Storhoff, J. J. *Nature* **1996**, *382*, 607–609.
(7) Alivisatos, A. P.; Johnsson, K. P.; Peng, X. G.; Wilson, T. E.; Loweth, C. J.; Bruchez, M. P.; Schultz, P. G. *Nature* **1996**, *382*, 609–611.
(8) Deng, Z. X.; Tian, Y.; Lee, S. H.; Ribbe, A. E.; Mao, C. D. *Angew. Chem., Int. Ed.* **2005**, *44*, 3582–3585.
(9) Sharma, J.; Chhabra, R.; Liu, Y.; Ke, Y.; Yan, H. *Angew. Chem., Int. Ed.* **2006**, *45*, 730–735.
(10) Chen, Y.; Liu, H. P.; Ye, T.; Kim, J.; Mao, C. D. *J. Am. Chem. Soc.* **2007**, *129*, 8696–8697.
(11) Lee, J. H.; Wernette, D. P.; Yigit, M. V.; Liu, J.; Wang, Z.; Lu, Y. *Angew. Chem., Int. Ed.* **2007**, *46*, 9006–9010.
(12) Lu, Y.; Liu, J. *Acc. Chem. Res.* **2007**, *40*, 315–323.
(13) Braun, E.; Eichen, Y.; Sivan, U.; Ben-Yoseph, G. *Nature* **1998**, *391*, 775–778.
(14) Shena, M.; Shalon, D.; Davis, R. W.; Brown, P. O. *Science* **1995**, *270*, 467–470.
(15) Yu, A.; Savas, T. A.; Taylor, G. S.; Guiseppe-Elie, A.; Smith, H. I.; Stellacci, F. *Nano Lett.* **2005**, *5*, 1061–1064.
(16) Akbulut, O.; Jung, J.; Bennett, R. D.; Hu, Y.; Jung, H.; Cohen, R. E.; Mayes, A. M.; Stellacci, F. *Nano Lett.* **2007**, *7*, 3493–3498.
(17) Lin, H.; Sun, L.; Crooks, R. M. *J. Am. Chem. Soc.* **2005**, *127*, 11210–11211.
(18) Thibault, C.; Berre, V. L.; Casimirius, S.; Trevisiol, E.; François, J.; Vieu, C. *J. Nanobiotechnol.* **2005**, *3*, 7.
(19) Lange, S. A.; Benes, V.; Kern, D. P.; Hörber, J. K.; Bernard, A. *Anal. Chem.* **2004**, *76*, 1641–1647.
(20) Dorota, I.; Rozkiewicz, I.; Brugman, W.; Kerkhoven, R. M.; Ravoo, B. J.; Reinhoudt, D. N. *J. Am. Chem. Soc.* **2007**, *129*, 11593–11599.
(21) Demers, L. M.; Ginger, D. S.; Park, S. J.; Li, Z.; Chung, S. W.; Mirkin, C. A. *Science* **2002**, *296*, 1836–1838.
(22) Chung, S.; Ginger, D. S.; Morales, M. W.; Zhang, Z.; Chandrasekhar, V.; Ratner, M. A.; Mirkin, C. A. *Small* **2005**, *1*, 64–69.
(23) Kim, K. H.; Sanedrin, R. G.; Ho, A. M.; Lee, S. W.; Moldovan, N.; Mirkin, C. A.; Espinosa, H. D. *Adv. Mater.* **2008**, *20*, 330–334.
(24) Bruckbauer, A.; Ying, L. M.; Rothery, A. M.; Zhou, D. J.; Shevchuk, A. I.; Abell, C.; Korchev, Y. E.; Klenerman, D. *J. Am. Chem. Soc.* **2002**, *124*, 8810–8811.
(25) Rodolfa, K. T.; Bruckbauer, A.; Zhou, D.; Korchev, Y. E.; Klenerman, D. *Angew. Chem., Int. Ed.* **2005**, *44*, 6854–6859.
(26) Okamoto, T.; Suzuki, T.; Yamamoto, N. *Nat. Biotechnol.* **2000**, *18*, 438–441.
(27) Butler, J. H.; Cronin, M.; Anderson, K. M.; Biddison, G. M.; Chatelain, F.; Cummer, M.; Davi, D. J.; Fisher, L.; Frauendorf, A. W.; Frueh, F. W.; Gjerstad, C.; Harper, T. F.; Kernahan, S. D.; Long, D. Q.; Pho, M.; Walker, J. A.; Brennan, T. M. *J. Am. Chem. Soc.* **2001**, *123*, 8887–8894.
(28) Hughes, T. R.; Mao, M.; Jones, A. R.; Burchard, J.; Marton, M. J.; Shannon, K. W.; Lefkowitz, S. M.; Ziman, M.; Schelter, J. M.; Meyer, M. R.; Kobayashi, S.; Davis, C.; Dai, H.; He, Y. D.; Stephaniants, S. B.; Cavet, G.; Walker, W. L.; West, A.; Coffey, E.; Shoemaker, D. D.; Stoughton, R.; Blanchard, A. P.; Friend, S. H.; Linsley, P. S. *Nat. Biotechnol.* **2001**, *19*, 342–347.
(29) Lausted, C. G.; Warren, C. B.; Hood, L. E.; Lasky, S. R. *Methods Enzymol.* **2006**, *410*, 168–189.
(30) Morozov, V. N.; Morozova, T. Y. *Anal. Chem.* **1999**, *71*, 3110–3117.
(31) Lee, J.; Cho, H.; Huh, N.; Ko, C.; Lee, W.; Jang, Y.; Lee, B. S.; Kang, I. S.; Choi, J. *Biosens. Bioelectron.* **2006**, *21*, 2240–2247.
(32) Konermann, L.; Silva, E. A.; Sogbein, O. F. *Anal. Chem.* **2001**, *73*, 4836–4844.
(33) Park, J.-U.; Hardy, M.; Kang, S. J.; Barton, K.; Adair, K.; Mukhopadhyay, D.; Lee, C. Y.; Strano, M. S.; Alleyne, A. G.; Georgiadis, J. G.; Ferreira, P. M.; Rogers, J. A. *Nat. Mater.* **2007**, *6*, 782–789.
(34) Sekitani, T.; Noguchi, Y.; Zschieschang, U.; Klauk, H.; Someya, T. *Proc. Natl. Acad. Sci. U.S.A.* **2008**, *105*, 4976–4980.
(35) Taylor, G. I. *Proc. R. Soc. London, Ser. A* **1969**, *313*, 453–475.
(36) Choi, H.; Park, J.-U.; Park, O.; Ferreira, F. M.; Georgiadis, J. G.; Rogers, J. A. *Appl. Phys. Lett.* **2008**, *92*, 123109.
(37) Voloshina, N. P.; Haugland, R. P.; Bishop-Stewart, J.; Bhalgat, M. K.; Millard, P. J.; Mao, F.; Leung, W.; Haugland, R. P. *J. Histochem. Cytochem.* **1999**, *47*, 1179–1188.
(38) Barbulovic-Nad, I.; Lucente, M.; Sun, Y.; Zhang, M.; Wheeler, A. R.; Bussmann, M. *Crit. Rev. Biotechnol.* **2006**, *26*, 237–259.
(39) Allain, L. R.; Stratis-Cullum, D. N.; Vo-Dinh, T. *Anal. Chim. Acta* **2004**, *518*, 77–85.
(40) Ellington, A. D.; Szostak, J. W. *Nature* **1990**, *346*, 818–822.
(41) Tuerk, C.; Gold, L. *Science* **1990**, *249*, 505–510.
(42) Breaker, R. R. *Nature* **2004**, *432*, 838–845.
(43) Liu, J.; Brown, A. K.; Meng, X.; Cropek, D. M.; Istok, J. D.; Watson, D. B.; Lu, Y. *Proc. Natl. Acad. Sci. U.S.A.* **2007**, *104*, 2056–2061.
(44) Lu, Y.; Liu, J. *Curr. Opin. Biotechnol.* **2006**, *17*, 580–588.
(45) Liu, J.; Lu, Y. *Angew. Chem., Int. Ed.* **2006**, *45*, 90–94.
(46) Yigit, M. V.; Mazumdar, D.; Lu, Y. *Bioconjugate Chem.* **2008**, *19*, 412–417.
(47) Collett, J. R.; Cho, E. J.; Ellington, A. D. *Methods* **2005**, *37*, 4–15.
(48) Nutiu, R.; Li, Y. *J. Am. Chem. Soc.* **2003**, *125*, 4771–4778.
(49) Demers, L. M.; Park, S.-J.; Taton, T. A.; Li, Z.; Mirkin, C. A. *Angew. Chem., Int. Ed.* **2001**, *40*, 3071–3073.
(50) Gerion, D.; Parak, W. J.; Williams, S. C.; Zanchet, D.; Micheel, C. M.; Alivisatos, A. P. *J. Am. Chem. Soc.* **2002**, *124*, 7070–7074.
(51) Liu, J.; Lu, Y. *Nat. Protoc.* **2006**, *1*, 246–252.

NL801832V